# Supplementary Information

# Imaging molecular crystal polymorphs and their polycrystalline microstructures *in situ* by ultralow-frequency Raman spectroscopy

Chun-Fu Chang,[a] Hajime Okajima,[ab] Hiro-o Hamaguchi[ac] and Shinsuke Shigeto*[a]

[a] *Department of Applied Chemistry and Institute of Molecular Science, National Chiao Tung University, Hsinchu 30010, Taiwan.*
[b] *Present address: Department of Chemistry and Biological Science, Aoyama-Gakuin University, Sagamihara 252-5258, Japan.*
[c] *Institute for Nanoscience and Nanotechnology, Waseda University, Tokyo 162-0041, Japan.*

* Corresponding author. E-mail: shigeto@mail.nctu.edu.tw; Fax: +886-3-572-3764; Tel: +886-3-571-2121

## Table of Contents

## Experimental Section

**Materials.** Powder 1,1′-binaphthyl (BN; 98% pure) was commercially obtained from Tokyo Chemical Industry. It was predominantly the cisoid form. To remove impurities and suppress fluorescence, the powder BN sample was first subjected to silica gel column chromatography with *n*-hexane as the eluent. The sample so purified was then used to grow single crystals of the cisoid form by gas diffusion recrystallization (Fig. S3a). It was dissolved in ethyl acetate in a small vial, which was placed in a larger vial containing *n*-pentane. Volatile *n*-pentane was allowed to diffuse into less volatile ethyl acetate, thus lowering the solubility of BN in the solution. As more and more volume of *n*-pentane mixed into ethyl acetate, apparent single crystals of cisoid BN were found on the wall of the small vial.

A piece of cisoid single crystal was transferred from the vial onto a microscope slide by a sharp needle made from a glass capillary. The glass needle took on static electricity on its surface, so that it attracted a tiny crystal gently. The sample was sandwiched with a cover slip, sealed with a heat-resistant tape, and kept on a hot plate at 130 °C for three days (Fig. S3b). After cooling down to room temperature, a number of microcrystals were observed under the microscope, which were identified as the transoid form of BN by using low-frequency (LF) Raman microspectroscopy (see Fig. 2b). Some of those microcrystals were isolated from the cisoid mother crystal, and some were attached on it. In this work, we studied one of the latter microcrystals.

**Confocal Raman microspectrometer for low-frequency measurements.** A schematic diagram of the confocal Raman microspectrometer that we have developed in the present study is shown in Fig. S2. The second harmonic (532 nm) of a cw Nd:$YVO_4$ laser (Verdi-V5, Coherent) was used as the excitation light. A small portion (<5%) of the output was directed to a high-resolution wavelength meter (WS-7, HighFinesse). Using this wavelength meter, the output wavelength was continuously monitored and maintained at 18789.902 $cm^{-1}$ with 60 MHz accuracy. After passing through an optical isolator and a polarizer, the laser beam was expanded by a factor of ~4.8. The expanded beam was then introduced to an inverted microscope (iX71, Olympus) and focused onto the sample by a long working-distance objective (20×, NA 0.45). The sample was placed on a 2-axis motorized stage (BIOS-Light, Sigma Koki). Back-scattered light was collected by the same objective, and focused by a secondary objective onto a pinhole with a 75 μm diameter to achieve confocal detection. The well-collimated scattered light was passed through two volume Bragg gratings[1] (BragGrate™ notch filters, OptiGrate), which eliminated virtually all Rayleigh scattering signal with LF Raman scattering intact. The elimination bandwidth is as narrow as 10 $cm^{-1}$. Using these VBGs, we were able to measure Raman signal at as low as ~10 cm$^{-1}$. The transmitted light was dispersed by a polychromator (f = 50 cm, *f*/6.5; SP-2558, Princeton Instruments) and detected by a liquid nitrogen-cooled CCD detector (Spec 10:400B, Princeton Instruments).

In our previous studies,[2] an iodine vapor cell was used as an ultranarrow notch filter instead of VBGs. VBGs have several advantages over the iodine vapor filter. First of all, they are free from spiky artifacts that always interfere with the raw Raman spectrum measured with the iodine vapor filter (Fig. S4, blue line). Second, they do not require any heating apparatus that is critical for sublimating solid iodine in the iodine vapor filter. Fig. S4 compares the transmittance of two VBGs and the iodine vapor filter operating at 60 °C, measured using white light from a tungsten lamp. The transmittance of two VBGs (Fig. S4, red line) is higher than 60% over the entire spectral range shown, whereas that of the iodine vapor filter (Fig. S4, blue line) is only ~40% with many spiky features. The major drawback of VBGs is that it has a relatively low Rayleigh-line blocking of OD 3 at the current state of technology. For the measurements of BN crystals, two VBGs were required to achieve sufficient elimination of Rayleigh scattered light. Another technical difficulty may arise from the keen sensitivity of VBGs to the angle of incidence, but this is not a serious problem in a confocal microscope system compared with an ordinary 90° scattering geometry (without a microscope).

To perform imaging experiments, the motorized stage mounted on the microscope stage was used to translate the sample in a raster manner. Acquisition of Raman spectra was synchronized with the sample translation using a LabVIEW (National Instruments) program.

The spectral resolution of our spectrometer was 2.7 cm$^{-1}$. Spatial resolution was estimated to be 1.5 (±0.1) μm in lateral (*XY*) direction and 32 (±1) μm in axial (*Z*) direction.

**Curve fitting analysis.** To construct Raman images shown in Fig. 1–3, the peak area of a given Raman band needs to be derived. To that end, we fit individual space-resolved Raman spectra (both Stokes and anti-Stokes regions) with the following function:[2a]

$$f(\tilde{\nu}) = y_0 + \left\{ \sum_{i=1}^{N} \left[ \frac{A_i \Gamma_i}{(\tilde{\nu} - \tilde{\nu}_i)^2 + \Gamma_i^2} + \frac{A_i \Gamma_i}{(\tilde{\nu} + \tilde{\nu}_i)^2 + \Gamma_i^2} \right] \right\} \times [1 + \exp(-hc\tilde{\nu}/k_{\mathrm{B}}T)]^{-1} \times (\tilde{\nu}_0 - \tilde{\nu})^3 \qquad (1)$$

Here $y_0$ accounts for a constant offset of the spectrum, $c$ is the speed of light, $h$ is Planck's constant, $k_{\mathrm{B}}$ is the Boltzmann constant, $T$ is absolute temperature, $\tilde{\nu}_0$ is the absolute wavenumber of the excitation light, and $\tilde{\nu}$ is Raman shift. The two terms in the square brackets represent Lorentzian functions for the Stokes and anti-Stokes Raman bands, respectively. $A_i$, $\Gamma_i$, and $\tilde{\nu}_i$ (> 0) denote peak area, width, and peak position, respectively, of the *i*th band. The accuracy in determination of these parameters is expected to be high because they are obtained from a pair of Stokes and anti-Stokes bands and not solely from the Stokes band. A different number of Lorentzian functions ($N$) was incorporated in Eq. 1, depending on the spectrum to be fitted. For instance, seven Lorentzian functions were used (i.e., $N = 7$) to fit the spectra shown in Fig. 1b. In fitting the high-frequency spectrum containing the 510 and 532 $\mathrm{cm}^{-1}$ bands, a superposition of two Voigt functions was used, solely for better estimation of the integrated area.

**Noise reduction using singular value decomposition.** To reduce noise in the spectra acquired in the polarized Raman experiment, a numerical preprocessing was performed using singular value decomposition[3] (SVD). SVD is a mathematical technique that factorizes an arbitrary $m \times n$ matrix $\boldsymbol{A}$ into the product of three matrices as $\boldsymbol{A} = \boldsymbol{U}\boldsymbol{W}\boldsymbol{V}^{\mathrm{T}}$. Here $\boldsymbol{U}$ is an $m \times n$ column-orthonormal matrix, $\boldsymbol{W}$ an $n \times n$ diagonal matrix of positive singular values, and $\boldsymbol{V}$ an $n \times n$ orthonormal matrix. In the present case, Raman spectra recorded at different positions in the sample consisted of the matrix $\boldsymbol{A}$, whose column corresponded to the spectrum at a particular measurement point and row carried position information. $\boldsymbol{U}$ and $\boldsymbol{V}$ represented the spectral and positional matrices, respectively. Components of $\boldsymbol{U}$ and $\boldsymbol{V}$ that had small singular values were neglected, because their contributions to the original data $\boldsymbol{A}$ would be negligibly small. The matrix $\boldsymbol{A}$ was then reconstructed by using only the components of $\boldsymbol{U}$ and $\boldsymbol{V}$ associated with large singular values. The number of singular values retained in this reconstruction was 10–20. The smallest singular value retained was about five orders of magnitude smaller than the largest singular value. The SVD was computed in Igor Pro (WaveMetrics).

## References

1 A. L. Glebov, O. Mokhun, A. Rapaport, S. Vergnole, V. Smimov and L. B. Glebov, *Proc. SPIE*, 2012, **8428**, 84280C.

2 (a) C.-F. Chang, S.-C. Wang and S. Shigeto, *J. Phys. Chem. C*, 2014, **118**, 2702; (b) H. Okajima and H. Hamaguchi, *Appl. Spectrosc.*, 2009, **63**, 958.

3 (a) N. Uzunbajakava, A. Lenferink, Y. Kraan, E. Volokhina, G. Vrensen, J. Greve and C. Otto, *Biophys. J.*, 2003, **84**, 3968; (b) H.-J. van Manen, Y. M. Kraan, D. Roos and C. Otto, *J. Phys. Chem. B*, 2004, **108**, 18762; (c) C.-K. Huang, H. Hamaguchi and S. Shigeto, *Chem. Commun.*, 2011, **47**, 9423.

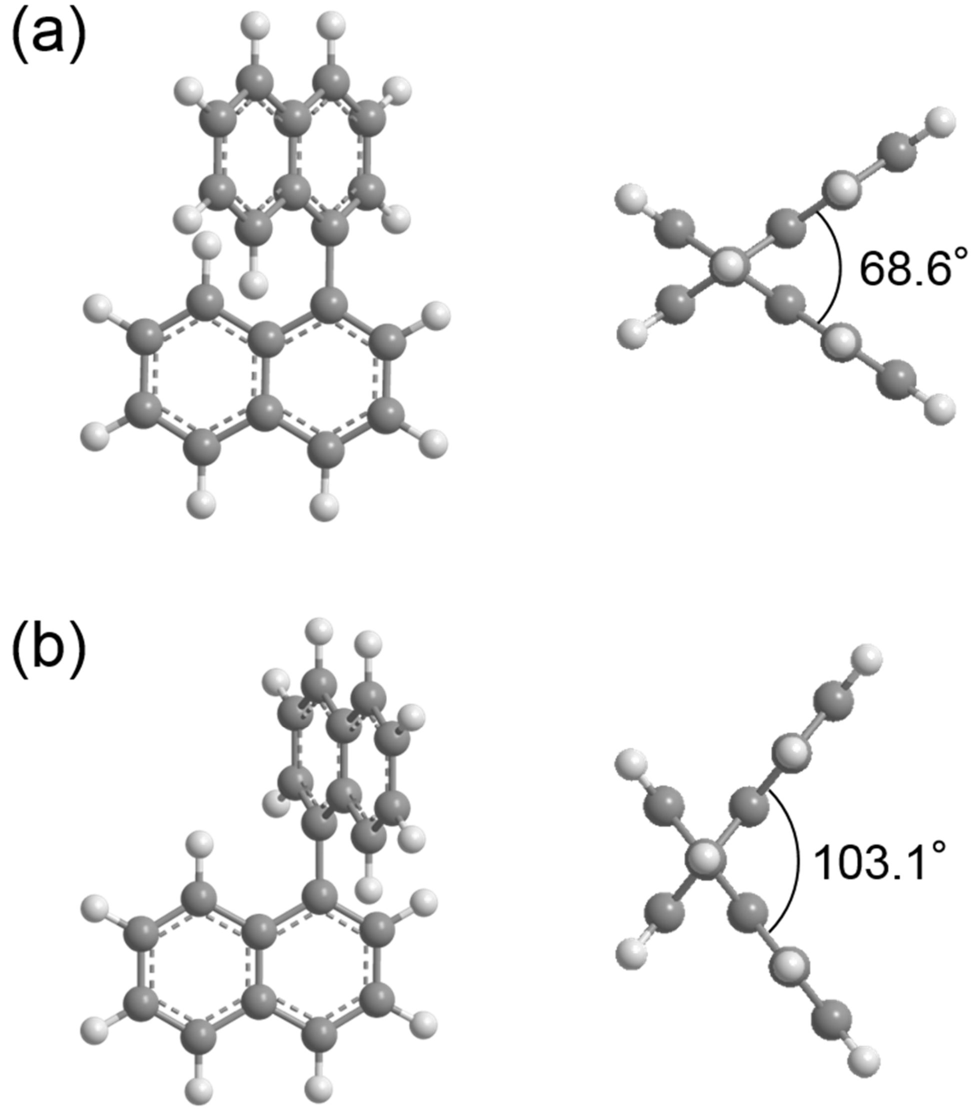

**Fig. S1** Molecular structure of the cisoid (a) and transoid (b) forms of BN. Shown on the right are the structures viewed along the inter-ring C–C single bond.

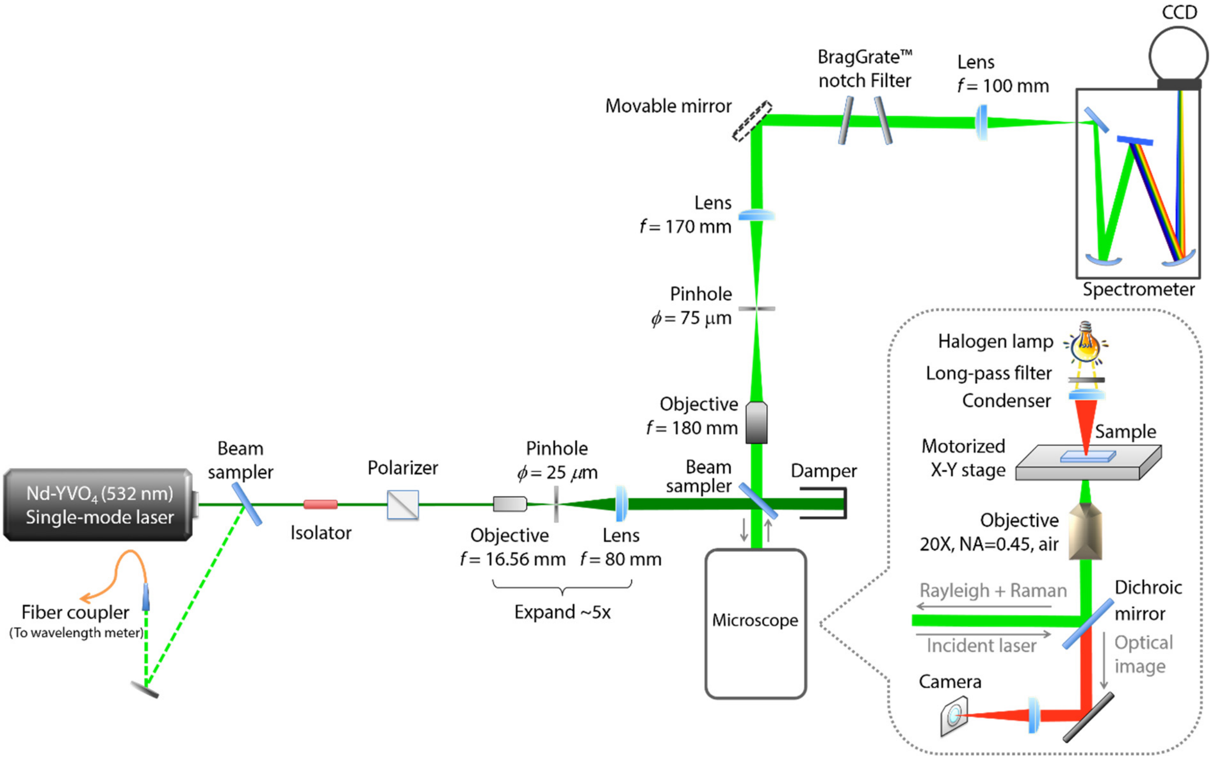

**Fig. S2** Schematic diagram of the laboratory-built confocal Raman microspectrometer that can measure an extremely low-frequency region (down to ca. ±10 cm$^{-1}$).

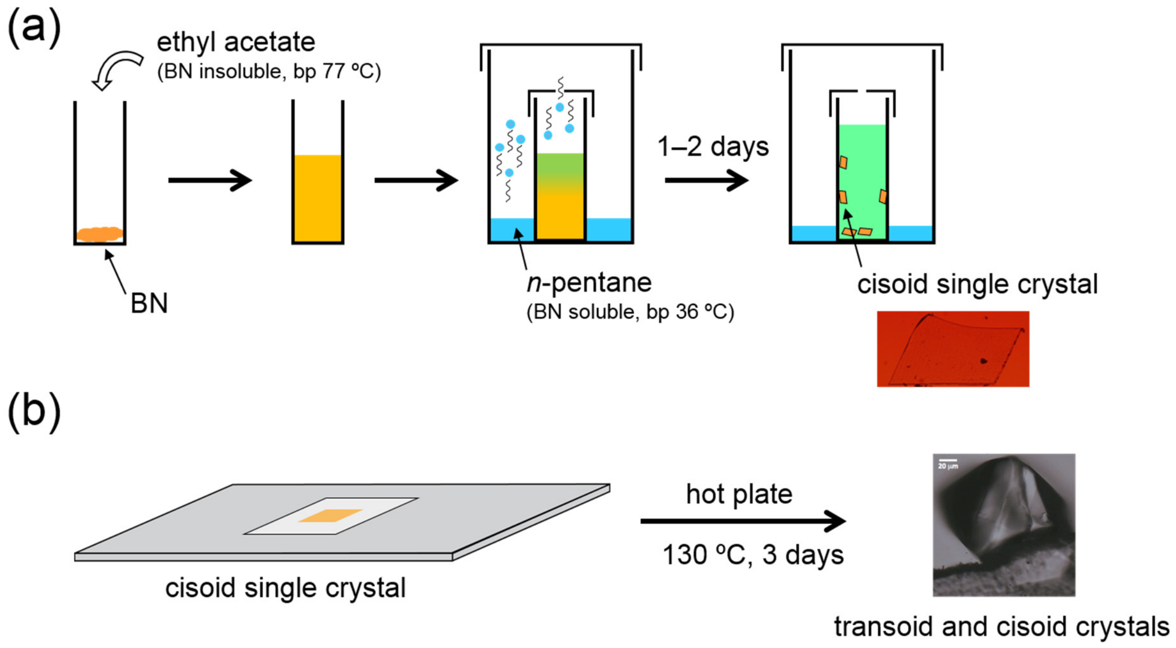

**Fig. S3** Preparation of cisoid (a) and transoid (b) crystals. See the Experimental Section above for details.

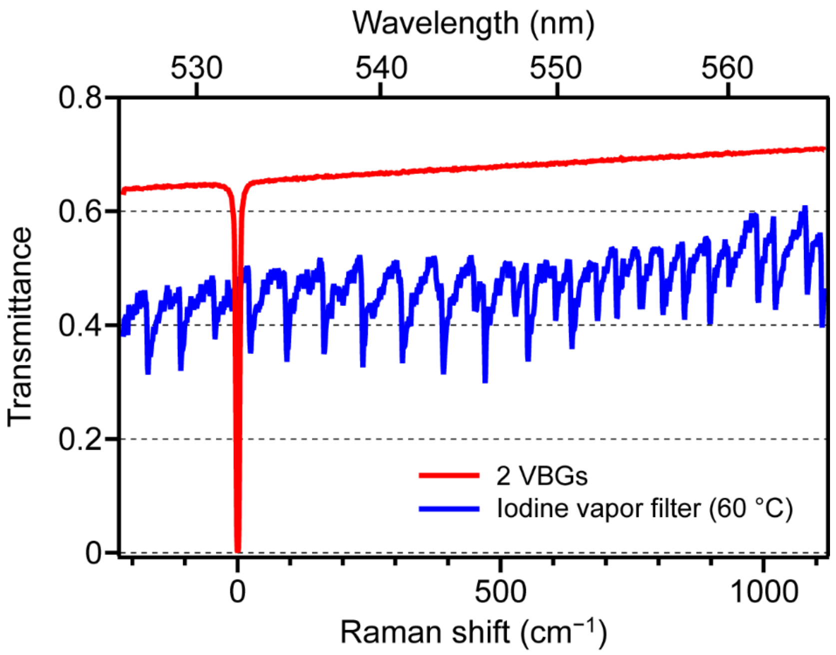

**Fig. S4** Transmittance curves of two VBGs (red) and the iodine vapor filter operating at 60 °C (blue) measured using white light from a tungsten lamp.

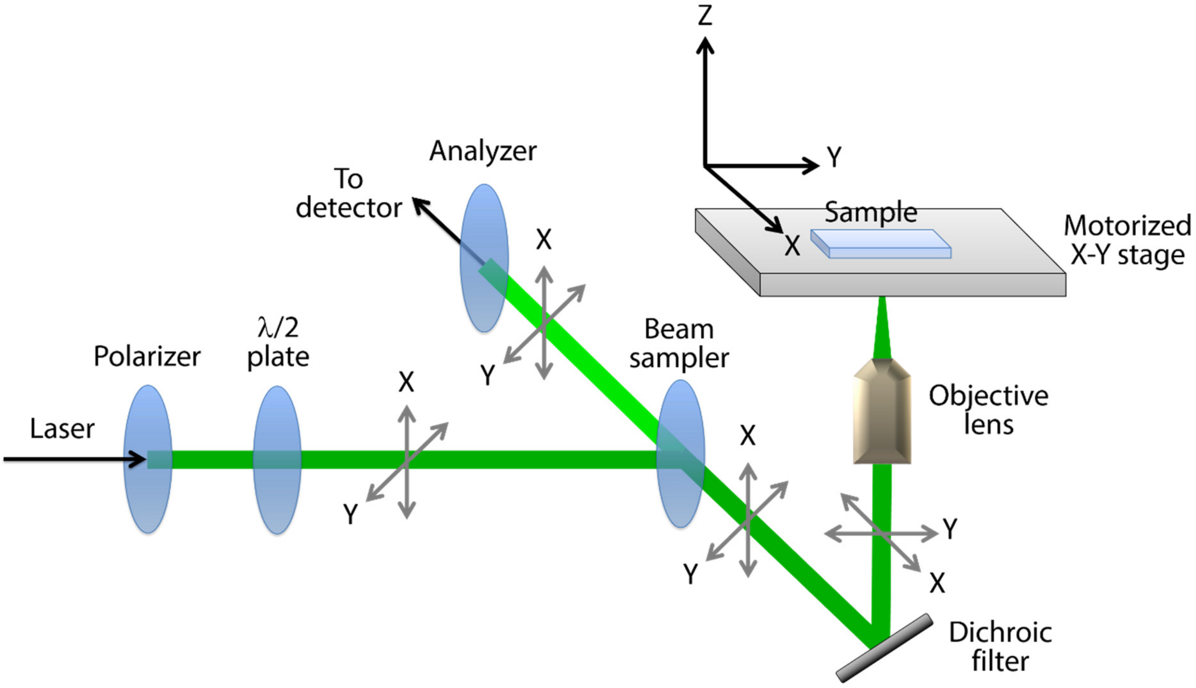

**Fig. S5** Schematic of the polarization configurations employed in the polarized Raman imaging experiment.